

# Evaluation of Cycle Performance of End-Plate Bolt Connections Based On Connection Parameters

Farzan Ekhlesi<sup>1</sup>, Hamid Saberi<sup>2</sup>, Vahid Saberi<sup>3</sup>

<sup>1</sup> Master of Science in Civil Engineering, University of Eyvanekey, Semnan, Iran

<sup>2</sup> Assistant Professor, Department of Civil Engineering, University of Eyvanekey, Semnan, Iran

**DOI: 10.46335/IJIES.2020.5.8.4**

**Abstract-** *The precise study of connections performance in a steel structure is important. End plate connections are commonly used in steel structures. In this research, the cyclic behavior of cantilever beam connection to the end-plate column under cyclic loading has been evaluated. In the calculations, all of the parameters affecting the behavior of this connection have been investigated and solutions are proposed to reach the maximum connection capacity. Two general models of connecting beams to different columns have been considered for the research with beams of 30 and 40 centimeters depth. The end plate thickness, end plate shape, column thickness, strength or the material of the bolt, necessity of using the continuity plate, double and gusset plate, are the parameters that were considered in the analyzes. According to the results of this study, the use of a thin end-plate causes localized buckling in the plate. The use of continuity plates is very important and prevents local buckling in the panel zone. It is also necessary to use a double plate if the column web is thin. Also, the use of gussets improves the flexural strength of the section.*

**Keywords-** *cyclic behavior, bolt connections, end plate, continuity plate, ductility.*

## I- INTRODUCTION

**D**ue to the increasing use of steel structures and the extended application of bolt connections, a careful examination of the connections performance in a steel structure is important, and inaccuracy in the design and implementation of connections not only causes failure in the joint, but also has devastating effects on other members of the structure. The beams and end plate set with embedded holes are connected to the column flange using high strength bolts in the workshop. There are two types of beam-column flange connections with named four-bolts and eight-bolts. The four-bolt connection is used for lower moment values and the eight-bolt connection for more bending moment values. In this research, the bending behavior of flange connection under increasing cyclic loading is evaluated by changing the effective parameters such as the end plate shape and the bolt material. For this purpose, several numerical models are prepared using finite element software and the extent of the effect of parameters on the flange connection behavior is determined. The main objective of this research is to investigate the bending behavior of end plate connection in steel structures under incremental cyclic loading by

varying parameters affecting the connection behavior, such as bolt, the use of stiffener (gusset), continuity plate and double plate. To this end, stress distribution in the connection components is investigated by changing the parameters and changing the position of the plastic joint in the beam and the bending capacity of the connection and the connection behavior based on hysteresis and rotational capacity and energy depletion. The results of this research can help to better design the flange bending connection.

This study evaluates the cyclic behavior of beam-column flange connection in steel frames using finite element analysis.

The ability to simulate the nonlinear behavior of the connection provides very high precision. In this connection, the steel beam is connected to the end plate using groove weld in flanges and groove or fillet weld in web with a suitable control. The set of beams and end plates in which holes are embedded, is attached to the column flange using high strength bolts.

Types of rigid connections used in steel structures include: rigid welded flange plate connection, rigid connection with straight welding of beam to column, rigid flange plate connection with 4 and 8 bolts, rigid end plate flange connection, flush and extended end-plate connections, with and without stiffener. In the flush end-plate connection, the dimensions of the end plate do not exceed the beam flange, but the extended end-plate connection, the dimensions of the end plate should exceed beam flange so that the bolt can be placed in the outer part of the plate. The extended end-plate connections can be with or without hardening between the tensile flange of the beam and the end plate on the web plate, which is used rigid connection of beam to column.

## **II- PREVIOUS RESEARCH**

Grundy et al. in 1980 [1] studied various parameters affecting the performance of flange connections. In their experiments, they measured three parameters, including the bolt diameter, the plate thickness and the column stiffener. Tsai and Popov in 1990 [2] tested three types of bending flange connection under a cyclic load using finite element analysis. The results show that the flange plate connections have excellent energy dissipation capacity. Hejazi and Mehdad in 2009 [3] investigated the effects of reinforcing plates on the flange connection of beam to the

column using finite element analysis. In this research, 6 numerical models were modeled using Ansys software. Based on the results obtained, the use of stiffener, especially triangular plates, significantly increases the ductility, rigidity and load bearing capacity of flanged connections. Joshi and colleagues in 2014 [4] modeled rigid flange connections using Abaqus software. The results of this study showed that, with increasing bolt diameter, the bending bearing capacity of the connection increases, and also the failure mode is located on the column flange.

Rajeshkumar et al. In 2013 [5] investigated the rigid flange connection under fire-induced heat. The modeling was performed using Abaqus finite element software different end plate thicknesses were evaluated. According to the results of this study, the increase in plate thickness, although increasing the flexural strength of the joint, increases the force in bolts and increases the risk of brittle fracture in the bolts. Balc In 2012 [6] investigated the beam connection to welded and bolted columns using numerical models. In this study, two samples of welded and bolted flange plates were analyzed using the finite element method in Abaqus software and the results were evaluated using laboratory data. Baei et al. In 2012 [7] presented a finite element modeling approach for numerical verification of the seismic performance of a rigid connection with bolted end plate, taking into account axial force. The results of the research showed that the presence of axial force affects the connection performance, so that the presence of the tensile force reduces the final bending strength of the joint. Ismail et al. In 2016 [8] examined the final performance of the end-plate steel connections. The results show that the non-stiffening model with flush end plate has a much lower bending strength than other models, and with increasing stiffening angle, the bending strength of the connection also increases. Saberi et.al In 2014,2016 [9] have explored comparison of bolted end plate and T-stub connection Sensivity to component thickness and bolt diameter on cyclic behavior. The result showed that The bolted T-stub connections are more sensitive to component thickness and bolt diameter rather than end plate connections. Moreover, they proposed using of post tensioned tendons for rehabilitation of mentioned weak connections. Dessouki et al. In 2013 [10] investigated the bending behavior of I-beam to end-plate connection in 2013. In this research,

Ansys software was used to analyze the parameters such as beam depth, plate thickness, bolt diameter, bolt thread, bolt strength and stiffness. Ghassemieh et al. In 2012 [11] used an artificial neural network supra-innovative algorithm to optimize the stiffened bending flange connection. Chen and Shi in 2016 [12] performed a finite elemental study on end plate bending connection for very high bending strength. In order to study the seismic behavior of bending frames with flange connections, a precise and effective finite element model under cyclic loading was prepared by Wang and colleagues in 2013 [13]. study the effect of retrofit parameters on cyclic behavior of bolted connections with weak end plate.

The analytical study is about the cyclic behavior of bolted connections with weak end plate retrofitted by welded haunches, the accuracy of modeling is verified by comparing the finite element model result with the experimental test results two specimens EP-R And EP-WP-H15-D30 that are tested by saberi et .al In 2017 [14] under SAC cyclic load .

Since end plate and beam are connected with complete joint penetration (CJP) groove and fillet welds, they are considered to be continuous in the FE model by Saberi et.al. In 2011 [15].

Saedi Daryan et. al. in 2012 [16] to consider interaction in contact surfaces of the connection, tangential behavior is defined by friction coulomb's coefficient of 0.3 and hard contact normal behavior. A pretension stress of 550Mpa is applied to all bolts.

In this research, both extended and flush flange connections were modeled and analyzed.

### III- RESEARCH METHODOLOGY

In this study, using nonlinear analyzes and finite element, several examples beam-column bolt connections with end-plate have been investigated. In this regard, static nonlinear analysis was performed using Abaqus software. With reliable modeling results from comparison of numerical and experimental results, effective parameters in the design of connections, such as the number of bolts and their placement, as well as the presence of stiffening agents, were investigated. For this purpose, two general models, including (A, a beam of 30 centimeters depth) and (B, a beam of 40 centimeters depth) are considered. Each

of A and B models are modeled and analyzed in different modes and their performance have been evaluated under cyclic loads. Various parameters have been investigated, such as the use of continuity plate, gusset plate, double plate, end plate thickness, end plate shape, column flange thickness and the bolt strength in the beam-column connection.

### IV-VERIFICATION

A laboratory research on connection with and without end plate stiffener was conducted under cyclic loads by Guo et al. In 2006 [17]. One of the samples tested in this research, named S-4 Sample (d), is considered for validation and modeling in Abaqus software.

The overall shape and dimensions of the members in the Guo test are as shown in Figure 1. The steel members of Q235B type steel are based on China standard, and the actual yield stress was found to be 310 MPa. M20 Bolts of 10.9 class with 960Mpa yield strength were used to connect the end plate to the column flange. For loading, first a 500 kN axial force corresponding to 20% of the column capacity was introduced. The cycling load was initially controlled by force. In the first two cycles, loading was applied to 20 kN and increased in the next cycles by 10 kN. This process continued until the connection reached the yield point. From this step, the loading was controlled by the displacement. The cyclic loading continues until the connection fails or the deviation is severe in the hysteresis curve. The details of the end plate are presented in Fig. 2.

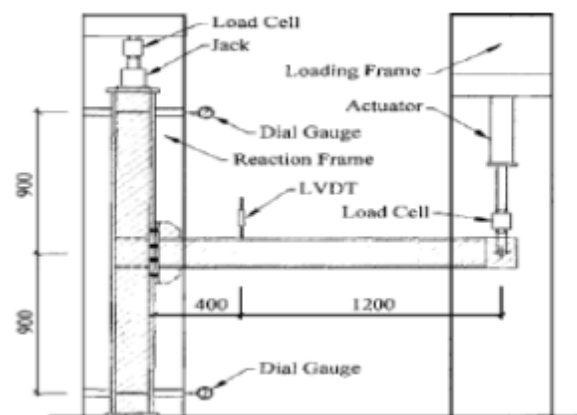


Fig. 1- General form of laboratory model [17].

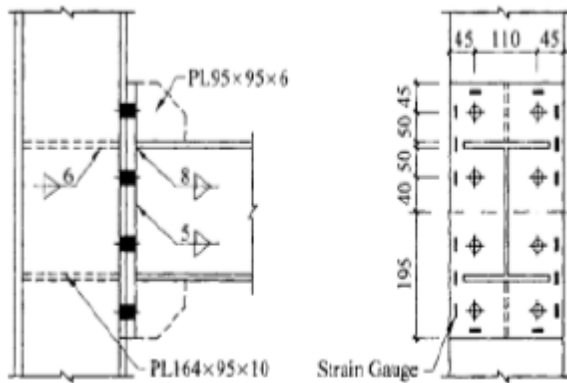


Fig. 2- End Plate details [17].

The specifications of beam and column used in the test and their bending capacity are presented in Table 1. The cross section of the beam and column are identical in all samples.

Members	Height (mm)	Flange Width (mm)	Flange Thickness (mm)	Web Thickness (mm)	Yield Moment (kNm)	Plastic Moment (kN.m)
Beam	200	150	10	6	93	103.4
Column	200	200	18	12	199.1	218.9

In Table 2, the specimen specifications are presented.

Table 2- Test Sample [17].

Column web continuity plate	Endplate Stiffener	Endplate thickness [mm]	Sample
No	No	18	S-4

All tested specimens have a rotational capacity of 0.033 to 0.072 radians. However, the difference between the failure states, the maximum moment and the energy dissipation capacity were significant among them. Abaqus finite element software is used to model the connection in 3D. Modeling was performed in 3D space, and different parts of the test prototype were simulated in the software model. The parts made in the model include steel beam, steel column, end plate, stiffener, continuity plate, bolt and nut. In accordance with the test process, first axial loading of

the column and then cyclic loading of the beam end is applied. The beam and column, end plate, and the stiffener are made of steel having a yield stress of 310 MPa, and a high strength steel of 960 MPa yield stress is used for bolts, also the friction coefficient considered to be 0.2.

The mechanical characteristics of the elements used in this modeling are presented in Tables 3 and 4.

Table 3- Specifications of steel used in analytical sample modeling.

Stress [MPa]	Strain	Location	Material
240	0.001143	Beam, Column, End-plate, Gusset plate, Continuity plate, Double plate	ST-37
240	0.02		
360	0.18		
370	0.20		
370	0.35		
360	0.001714	End plate	ST-52
360	0.005468		
380	0.007985		
398	0.012324		
415	0.019732		
433	0.031543		
450	0.049096		
468	0.073645		
485	0.106266		
503	0.147266		
520	0.19861		

Table 4- Bolts used in analytical sample modeling.

Stress [MPa]	Strain	Location	Material
794	0.00386	Bolt	10.9
1035	0.0135		
1035	0.0309		
1048	0.20	Bolt	8.8
640	0		
800	0.038		
800	0.148		

### V-VERIFICATION RESULT

The moment-rotation hysterical curve obtained from numerical modeling and corresponding curve obtained from the experimental model are shown in Figures 3 and 4.

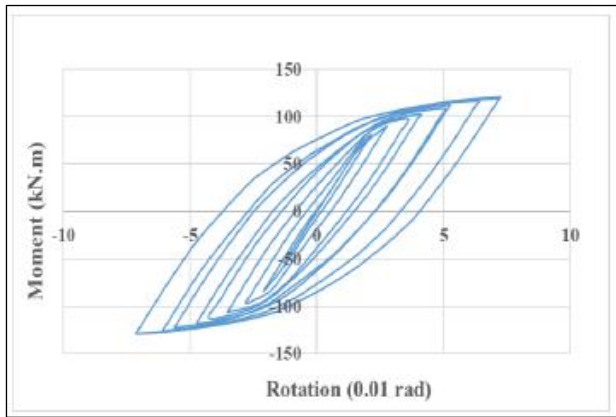


Fig. 3- Moment-rotation curve obtained from numerical modeling in Abaqus

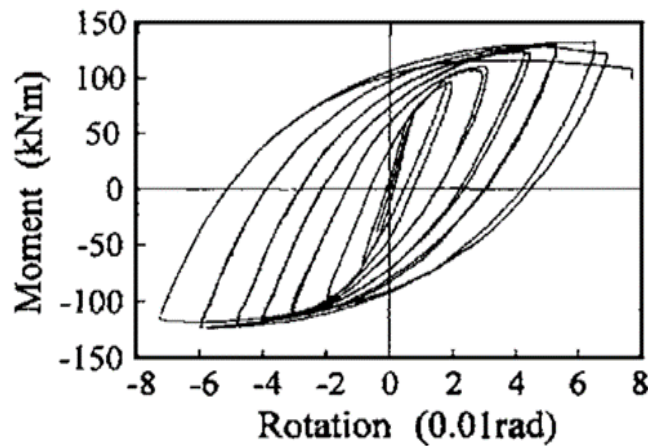


Fig. 4- Moment-rotation curve obtained from Guo test [17]

The comparison of the moment-rotation curve obtained from numerical modeling in Abaqus with the moment-rotation curve obtained from the Guo experiment is presented in Fig.5.

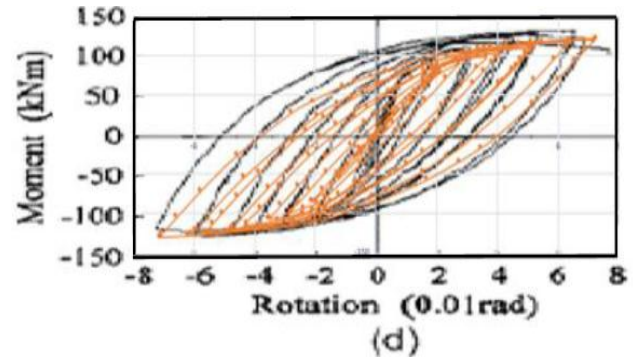


Fig. 5- Moment-rotation curve drawn from numerical modeling in Abaqus and Guo experiment [17].

As shown in Fig. 5, a finite element model can predict the behavior of the experimental model properly. The maximum bending moment obtained from the test is 123 kN . m and the maximum bending moment in the finite element model is 125 kN . m.

As shown in Fig. 6, in this model, the local buckling of the end plate and column wing have occurred.

The rotation that leads to failure is 0.07 radians.

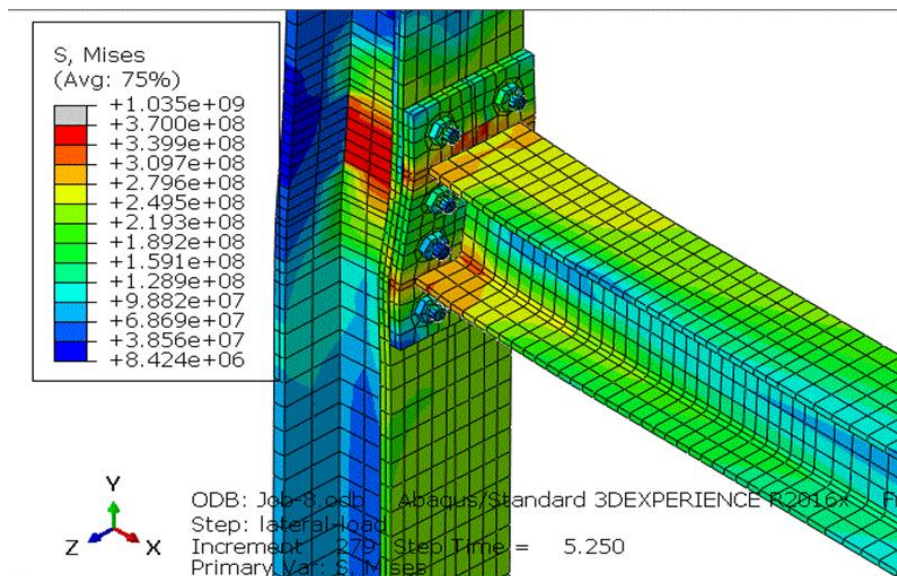


Fig. 6- Tension and deformation contour in the verification model

VI- INTRODUCING THE STUDIED MODELS

To perform this research, two general models have been considered, including (A, a beam of 30 centimeters depth) and (B, a beam of 40 centimeters depth). Each A and B model is modeled and analyzed in different modes and their performance is evaluated under cyclic loading. Various parameters such as the use of continuity plate, gusset plate, double plate, end plate thickness, the end plate shape, column flange thickness and the bolt strength in the beam- column end-plate connection are investigated.

The beam and column sections used in models A and B are shown in Figures 7 and 8.

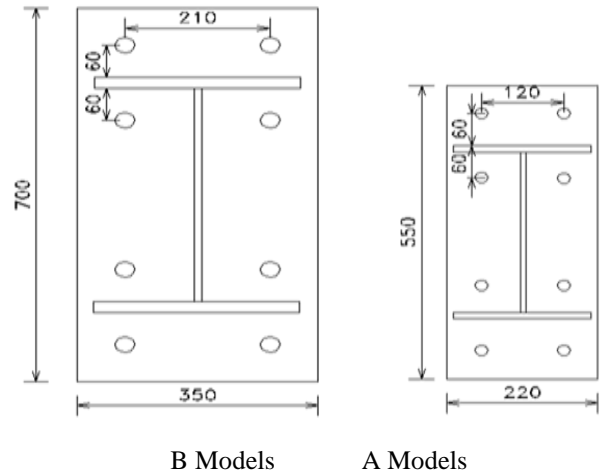


Fig. 9- Specifications for the end plates of the examined models

The setup of models A and B is shown in Figures 10 and 11.

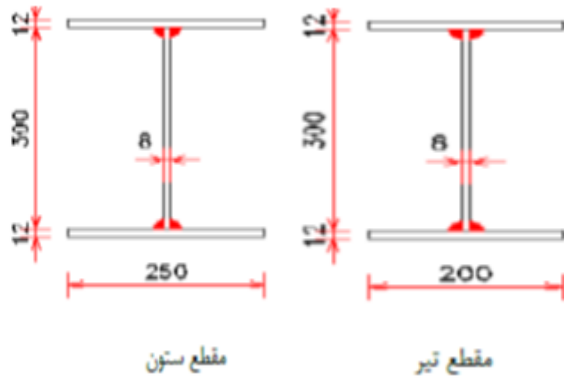


Fig. 7- Cross section of the beam and column (model A)

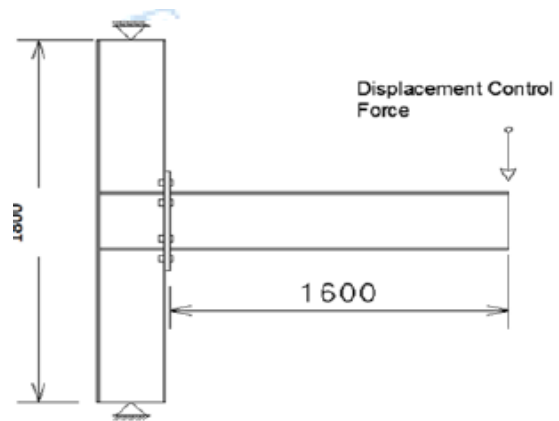


Fig. 10- Setup of A Models

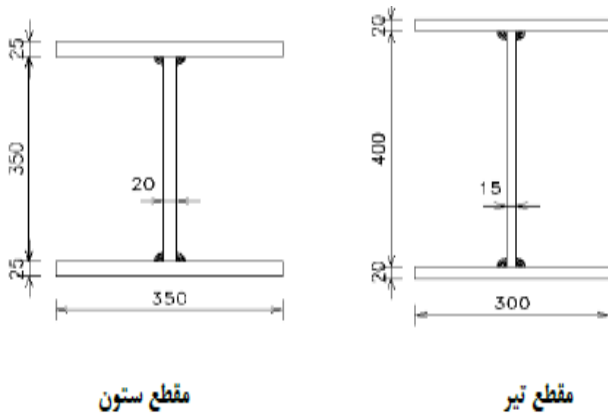


Fig. 8- Cross section of the beam and column (model B)

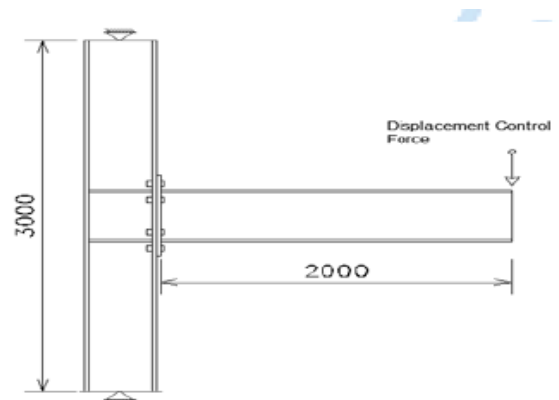


Fig. 11- Setup of B Models

The specifications of the end plates of models A and B are shown in Fig. 9.

In Tables 5 and 6, the specifications and parameters are presented in each model.

Table 5- Specifications of A Models.

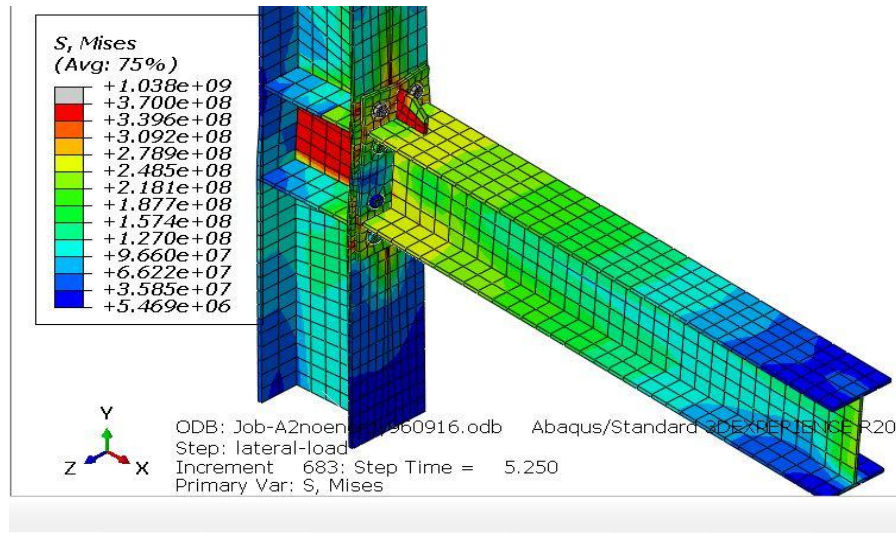
Model	Endplate thickness [mm]	Column flange thickness [mm]	Bolt material	Gusset plate	Gusset plate thickness [mm]	Continuity plate	Continuity plate thickness [mm]	Double plate	Double plate thickness [mm]
A0 ST-37	10	12	High strength	-	-	-	-	-	-
A1 ST-37	15	12	High strength	-	-	-	-	-	-
A2 ST-37	15	12	High strength	Yes	12	Yes	12	-	-
A3 ST-37	20	12	High strength	Yes	20	Yes	12	Yes	8
A4 ST-37	20	20	High strength	Yes	20	Yes	12	Yes	8
A1 ST-52	15	12	High strength	-	-	-	-	-	-
A4 ST-52	20	20	High strength	Yes	20	Yes	12	Yes	8

Table 6- Specifications of B Models.

Model	Endplate thickness [mm]	Column flange thickness [mm]	Bolt material	Gusset plate	Gusset plate thickness [mm]	Continuity plate	Continuity plate thickness [mm]
B1 ST-37	30	25	Conventional	-	-	-	-
B2 ST-37	30	25	High strength	-	-	-	-
B3 ST-37	30	25	High strength	Yes	25	Yes	20
B3 ST-52	30	25	High strength	Yes	25	Yes	20

It should be noted that in connection A, the plastic moment of the beam is 300 kN.m. In connection B, the plastic moment of the beam is 1000 kN.m.





- A3 S

In this model, the yield of the column flange remains the weak point of this connection.

The rotation that leads to failure is 0.06 radians.

- A4 ST-37 Model

As shown in Fig. 14, in this model nonlinear behavior is completely transmitted to the beam.

The rotation that results in failure is 0.057 radians.

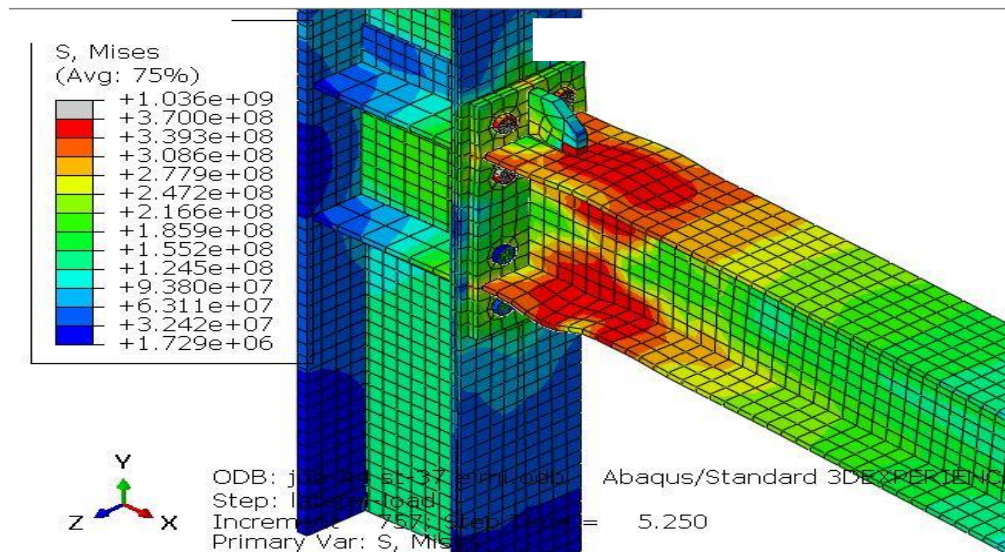


Fig. 14- Tension and deformation contour in the A4 ST-37 model

- A4 ST-52 Model

In this model, the nonlinear behavior is completely transmitted to the beam.

The rotation that causes failure is 0.068 radians.

- B1 ST-37 Model

As shown in Figure 15, failure has occurred due to a fracture of the bolt.

The rotation that results in failure is 0.056 radians

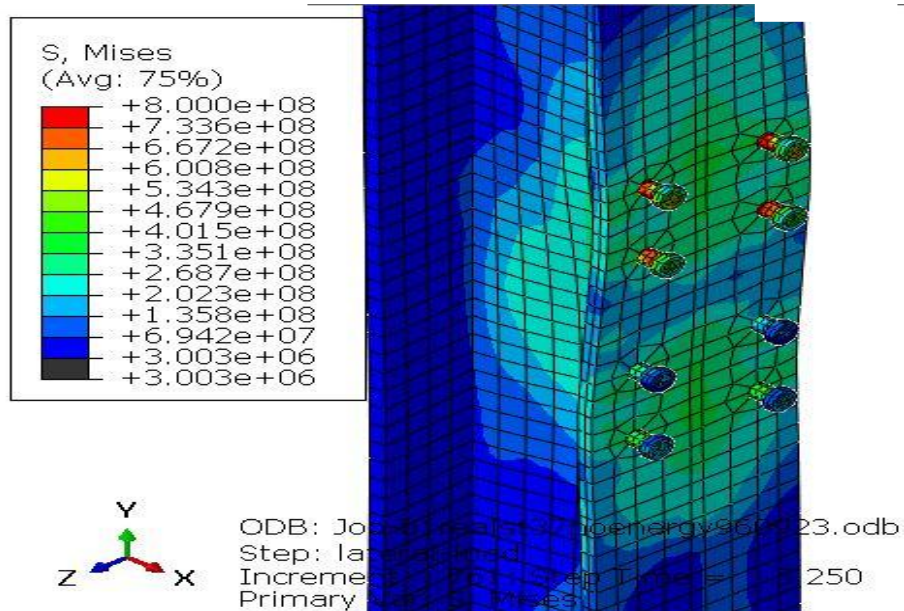


Fig. 15- Tension and deformation contour in the B1 ST-37 model

- B2 ST-37 Model

As shown in Fig. 16, in this model, the failure has occurred due to the local buckling of the column web and flange. The rotation that causes failure is 0.054 radians.

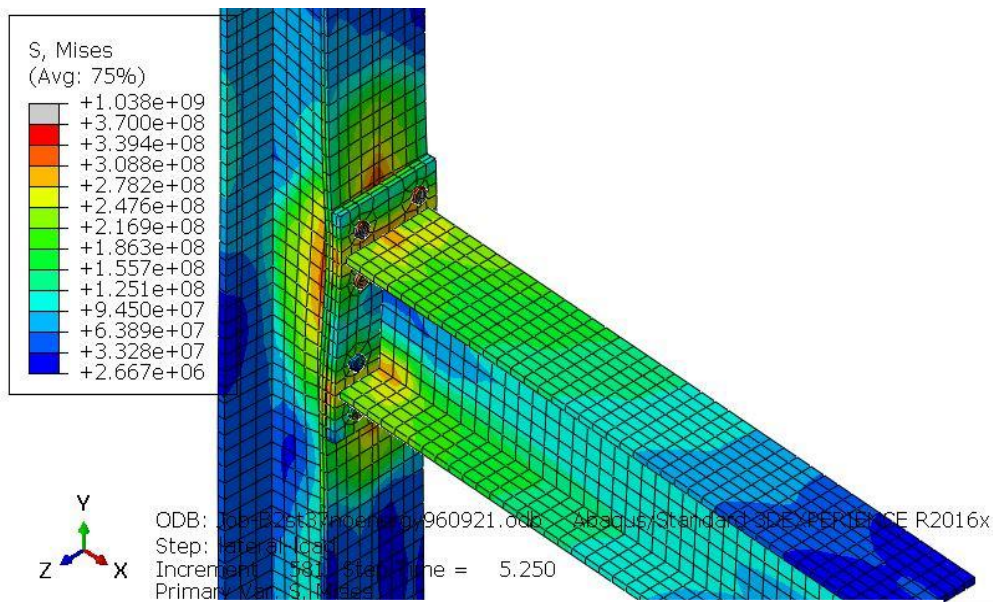
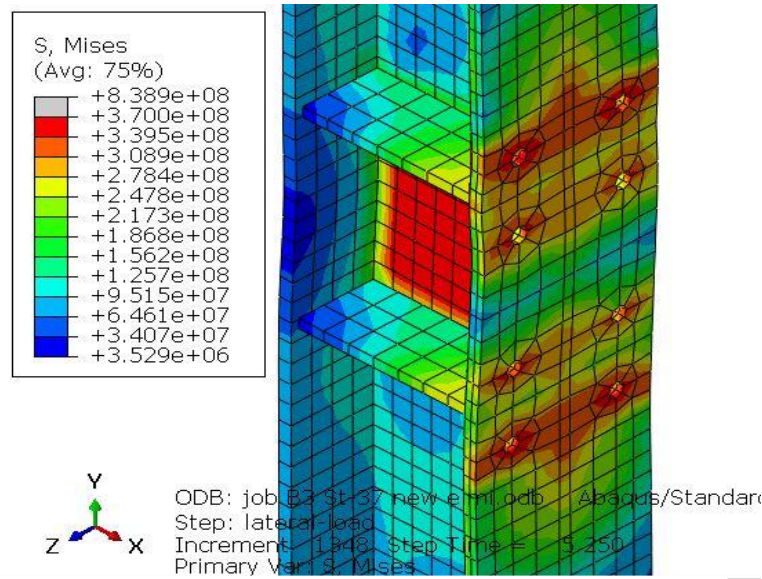


Fig. 16- Tension and deformation contour in model B2 ST-37

**- B3 ST-37 Model**

As shown in Figures 17 and 18, yield has occurred in the gusset plate and around the hole and the panel zone.

The rotation that leads to failure is 0.048 radians.



**Fig. 17- Tension and deformation contour in B3 ST-37 model**

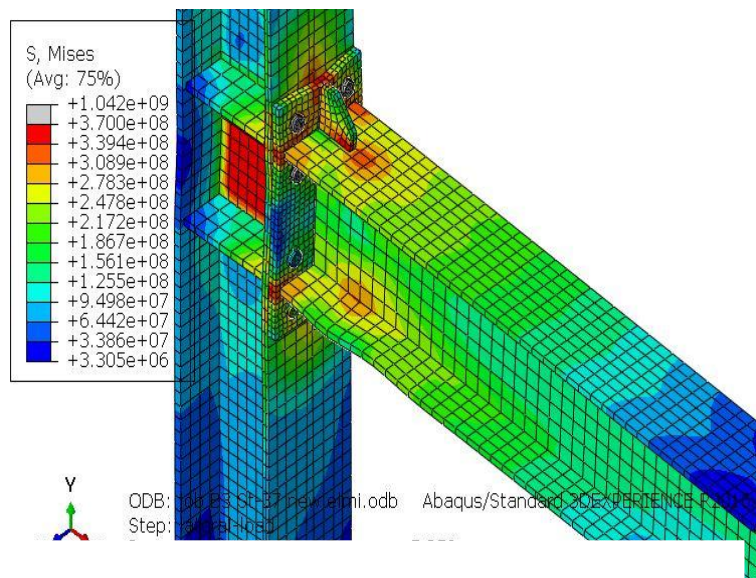


**Fig. 18- Tension and deformation contour in B3 ST-37 model**

**- B3 ST-52 Model**

In this model, yield has occurred in the gusset plate and around the hole and the panel zone.

The rotation that leads to failure is 0.054 radians

VIII - DISCUSSION ON THE RESULTS

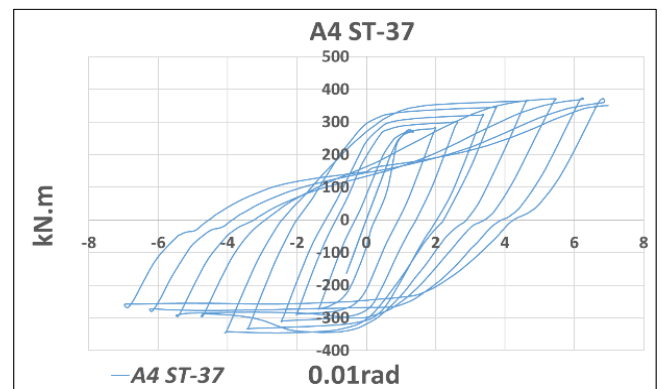
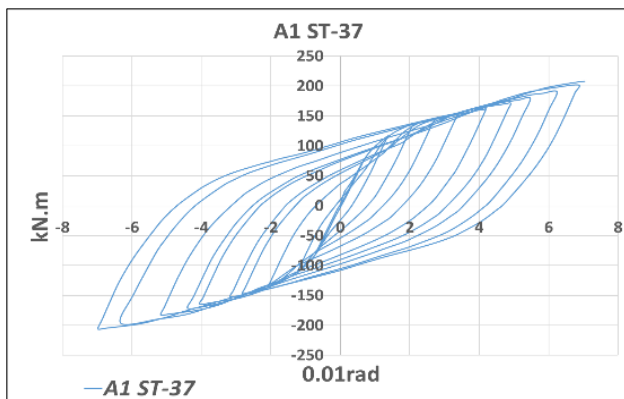
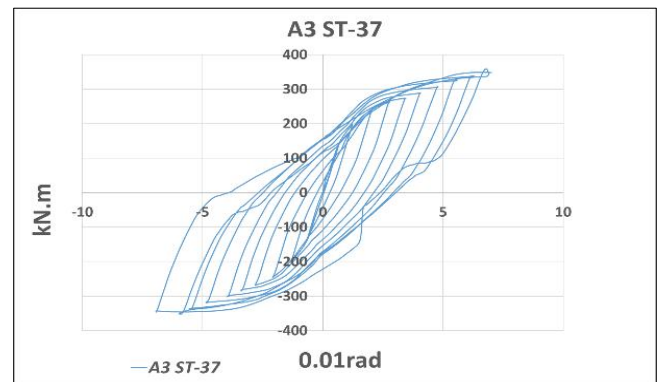
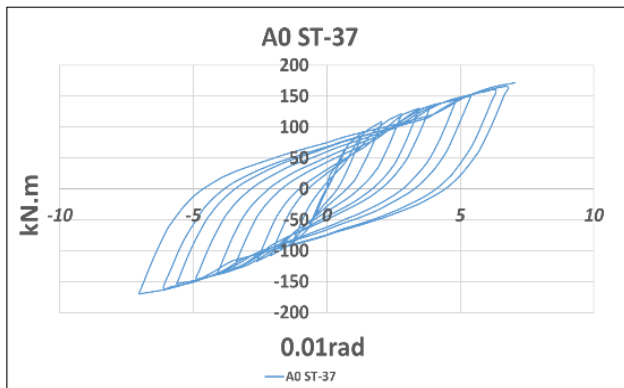
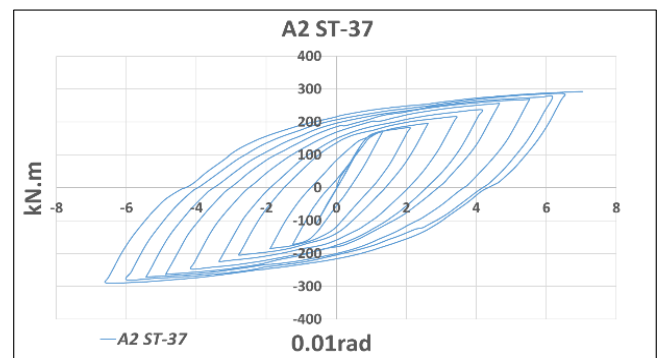
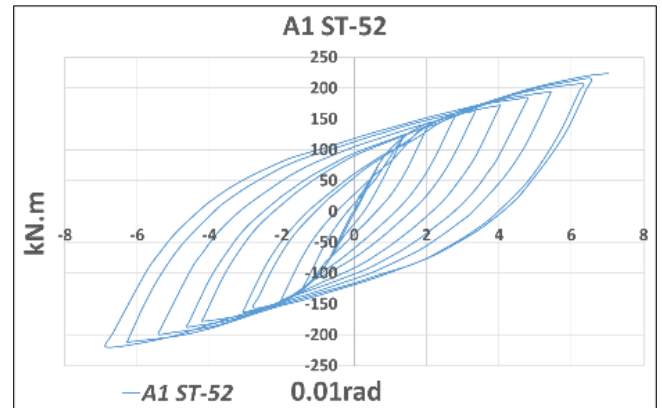
1 – 1 Bending capacity and bending behavior of connections

Table 7 shows the comparison between the models A0 ST-37 to A4 ST-37, as well as A1 ST-52 and A4 ST-52 models in terms of bending capacity.

Table 7- Flexural Capacity of Samples A.

Samples	Connection Flexural Capacity [kN.m]
A0 ST-37	172
A1 ST-37	208
A2 ST-37	292
A3 ST-37	358
A4 ST-37	373
A1 ST-52	224
A4 ST-52	380

Moment-rotation hysteresis diagrams of samples A are shown in Fig. 19.



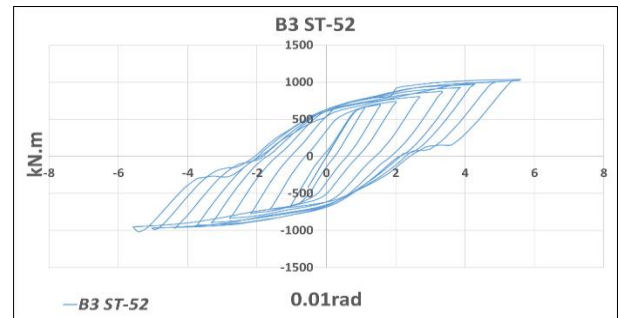
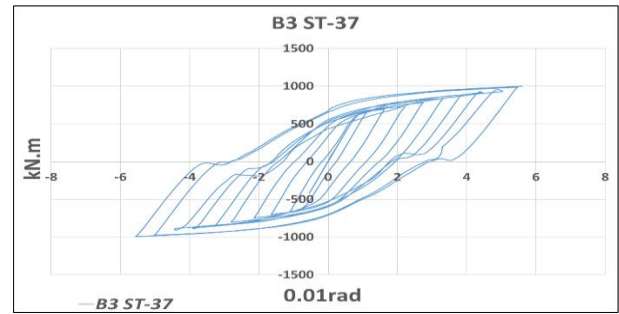
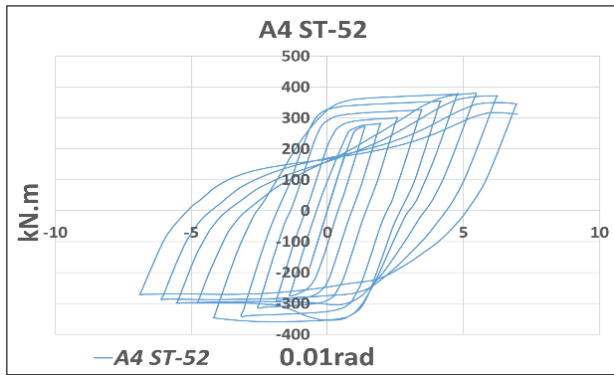


Fig. 19- Moment-rotation hysteresis diagrams of A Models

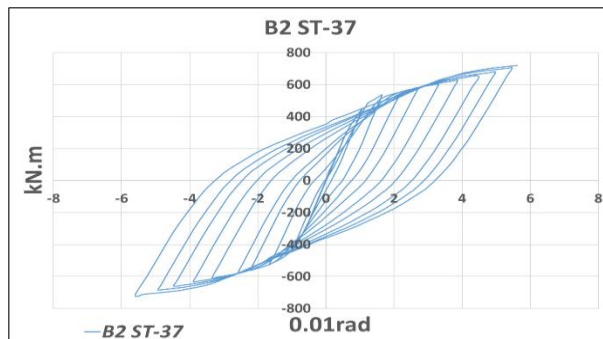
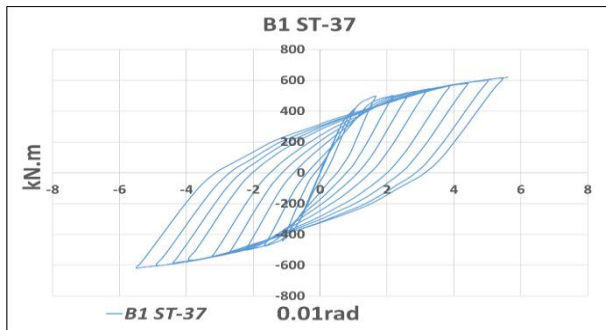
Table 8 shows the comparison between B1 ST-37 to B3 ST-37 models as well as the B3 ST-52 model in terms of connection bending capacity.

Table 8- Bending Capacity of Samples B.

Samples	Connection Flexural Capacity [kN.m]
B1 ST-37	619
B2 ST-37	720
B3 ST-37	1010
B3 ST-52	1036

Moment-rotation hysteresis diagrams of samples B are shown in Figure 20.

Fig. 20- Moment-rotation hysteresis diagrams of B Models



### 1-2 Examination of the rotational stiffness of the connections

To calculate the rotational stiffness, first, the pushover curve is made double-linear and the intersection of the first and second lines is placed on the rotation-yield moment graph and the rotational stiffness is obtained by dividing yield moment to yield rotation.

The envelope curve of the moment-rotation hysteresis diagrams for A1 ST-37 to A4 ST-37 models, as well as A1 ST-52 and A4 ST-52 models is shown in Fig. 21.

Meanwhile, the A0 ST-37 model, which has no gusset, continuity and double plate, having a rotational stiffness of 9200 kN.m/rad has the lowest initial stiffness and the A4 ST-37 model with a rotational stiffness of 25400 kN.m/rad has the highest initial stiffness. It is completely clear that the addition of gusset, continuity and double plate, as well as increasing the thickness of the connection plate to provide the minimum required thickness, increases the rotational stiffness. The use of ST-52 steel has also increased the rotational stiffness of the A1 ST-52 model. The A1 ST-52 rotational stiffness has risen 3 percent compared to the A1 ST-37 model, and the rotational stiffness of the A4 ST-52 model has increased by 3 percent compared to A4 ST-37.

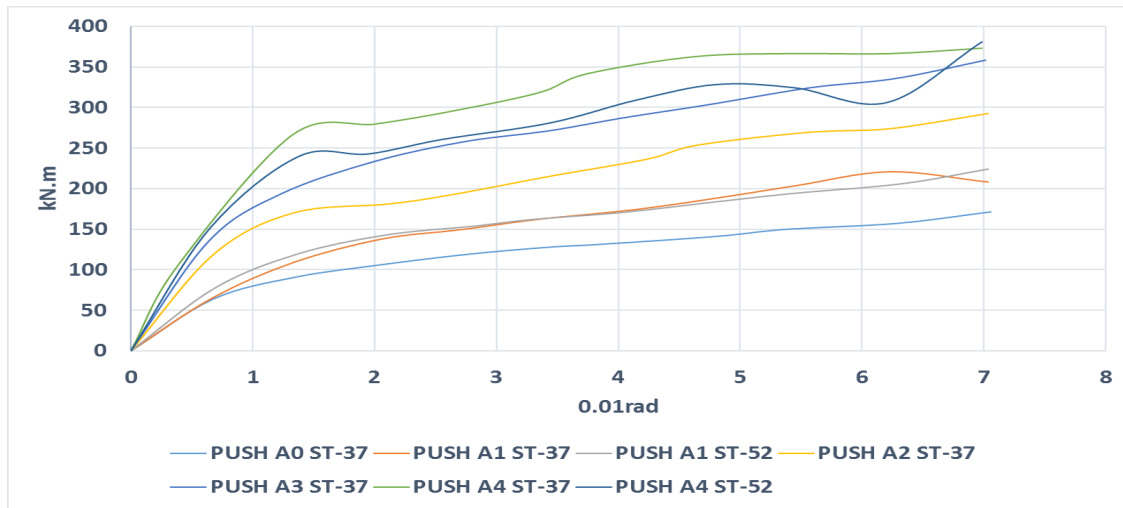


Fig. 21- Moment-rotation hysteresis curve - A1 ST-37 to A4 ST-37, A1 ST-52, A4 ST-52 models

Table 9 shows the comparison between A0 ST-37 to A4 ST-37 models as well as A1 ST-52 and A4 ST-52 models in terms of rotational stiffness.

Table 9- Rotational stiffness of samples A.

Samples	Connection Rotational Stiffness [kN.m/rad]
A0 ST-37	9200
A1 ST-37	11300
A2 ST-37	18300
A3 ST-37	19900
A4 ST-37	25400
A1 ST-52	11600
A4 ST-52	26000

The envelope of the moment-rotation hysteresis diagrams of B1 ST-37 to B3 ST-37 models as well as the B3 ST-52 model is shown in Fig. 22. The B1 ST-37 model, with no gusset and continuity plate and a conventional bolt, has a rotational stiffness of 40170 kN.m/rad with the lowest rotational stiffness and the B3 ST-37 model with a rotational stiffness 72500 kN.m/rad has the highest rotational stiffness. The use of a high strength bolt rather than a regular bolt does not have much impact on rotational stiffness, but the use of gusset and continuity plate can increase the rotational stiffness. Also, the use of ST-52 steel on the end plate has increased the rotational stiffness of the B3 ST-52 model.

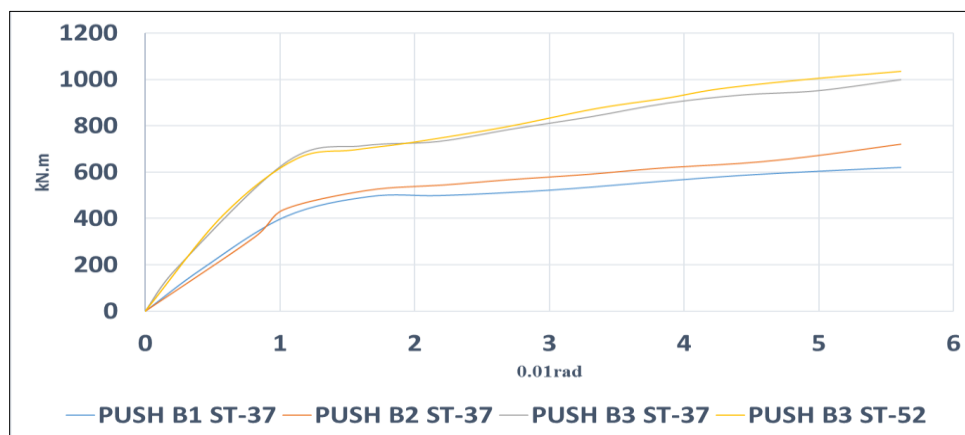


Fig. 22- Envelope of moment-rotation hysteresis curve - B1 ST-37 to B3 ST-37 , B3 ST-52 models

Table 10 shows the comparison between B1 ST-37 to B3 ST-37 models as well as the B3 ST-52 model in terms of rotational stiffness:

Table 10- Rotational stiffness of samples B

Samples	Connection Rotational Stiffness [kN.m/rad]
B1 ST-37	40170
B2 ST-37	42000
B3 ST-37	72500
B3 ST-52	73660

1 – 3 Energy absorption study

The energy absorption of A0 ST-37 to A4 ST-37 models, as well as A1 ST-52 and A4 ST-52 models, is shown in Fig. 23.

Energy absorption in the A4 ST-37 model is more than A0 ST-37 and A1 ST-37 models. This is due to the larger and more complete hysteresis loops, as well as plastic moment capacity of the beam and the formation of plastic connection in the beam in the A4 ST-37 model.

The A0 ST-37 and A1 ST-37 models the reason for low energy absorption is due to low plastic deformation and early failure.

The energy absorption of the A1 ST-52 and A4 ST-52 models is more than the A1 ST-37 and A4 ST-37 models, due to the use of ST-52 steel in the end plate.

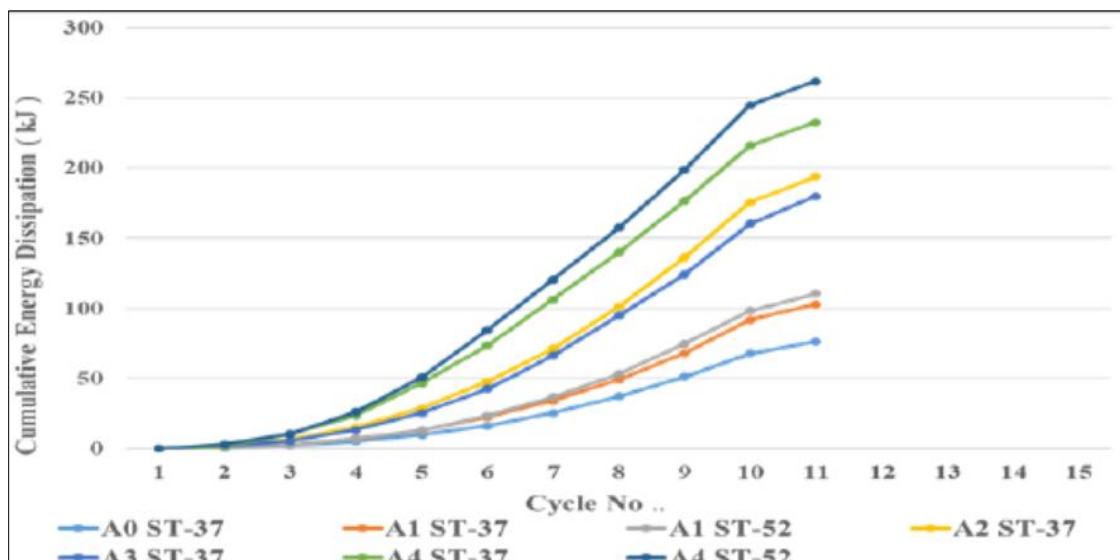


Fig. 23- Energy absorption in A0 ST-37 to A4 ST-37, A1 ST-52, A4 ST-52 models

Table 11 shows the comparison between A0 ST-37 to A4 ST-37 models as well as A1 ST-52 and A4 ST-52 models in terms of energy absorption.

Table 11- Energy absorption of samples A.

Samples	Connection Energy Absorption [kJ]
A0 ST-37	76
A1 ST-37	103
A2 ST-37	194
A3 ST-37	215

A4 ST-37	233
A1 ST-52	110
A4 ST-52	262

The energy absorption in B1 ST-37 to B3 ST-37 and B3 ST-52 models is shown in Figure 24. Energy absorption in the B3 ST-37 model is more than the B1 ST-37 and B2 ST-37 models. Because the use of continuity plate prevents buckling on the column flange, and hysteresis loops are more complete in the B3 ST-37 model, and ultimately, higher energy absorption is provided.

The B1 ST-37 and B2-ST-37 models were the reason for low energy absorption due to low plastic deformation and early failure.

The use of ST-52 steel also increased energy absorption and caused 19% increase in energy absorption in the B3 ST-52 model compared to the B3 ST-37 model.

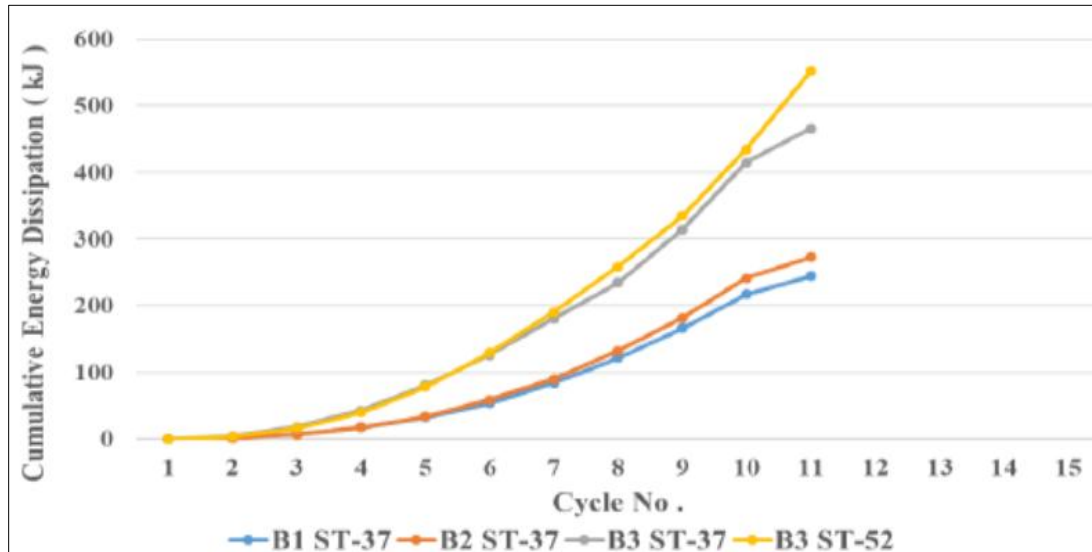


Fig. 24- Energy absorption in B1 ST-37 to B3 ST-37, B3 ST-52 models

Table 12 shows the comparison between B1 ST-37 to B3 ST-37 and B3 ST-52 models in terms of energy absorption:

Table 12- Energy absorption of samples B.

Samples	Connection Energy Absorption [kJ]
B1 ST-37	244
B2 ST-37	273
B3 ST-37	466
B3 ST-52	552

### IX- CONCLUSION

The connection A refers to the beam with plastic moment of 300 kN.m. In the A0 ST-37 model, which lacks a continuity plate and sufficient thickness for the connection plate, the bending capacity is 172 kN.m. Using a suitable thickness plate, the connection capacity reaches 208 kN.m, but the local buckling of the column flange prevents proper hysteresis behavior. In this case, the use of continuity and gusset plates has improved nonlinear

behavior and increased connection strength to 292 kN.m. But still the yield of panel zone and column flange due to low thickness is the main reason for failure in this connection. By adding a double plate to reinforce the panel zone and also increasing the column flange thickness, the connection capacity reached 373 kN. m and complete hysteresis loops were achieved. In this case, nonlinear behavior occurs entirely in the beam and energy absorption reaches the maximum value. Also, the use of ST-52 steel has increased bending capacity. In the A1 ST-52 model, the bending capacity is 224 kN.m, which is 8% higher than the A1 ST-37, and In the A4 ST-52 model, the bending capacity is 380 kN.m, which is 3% higher than the A4 ST-37

The connection B refers to the beam with plastic moment of 1000 kN.m. In the B1 ST-37 model, which uses a conventional bolt without stiffener and continuity plate, the bending strength is 619 kN.m. The use of a high strength bolt yielded a bending strength of 720 kN.m, but the hysteresis behavior was improper and failure occurred in the column. Moreover, the use of a continuity plate and stiffener (gusset) increases the bending capacity to 1010 kN.m. In this case, the hysteresis loops are more complete,

and failure due to the yield of the beam and the panel zone occurred.

Also the use of ST-52 steel has increased the bending capacity to 1036 kN.m in B3 ST-52 sample, which is 4% higher than that of the B3 ST-37 sample.

By examining the results, with respect to plastic moment of the beam and failure moment of connection, the optimum model includes A4 ST-37 in A models with 20 mm thickness of end plate, 20 mm column flange thickness, 20 mm gusset plate thickness, 12 mm continuity plate thickness and 8 mm thickness of double plate, as well as B3 ST-37 model in B models with 30 mm end plate thickness, 25 mm column flange thickness, 25 mm gusset plate thickness and 20 mm continuity plate thickness.

Some of the most important results from this research are as follows:

- The use of a continuity plate has a significant effect on preventing the local buckling of the column flange and web, which improves the nonlinear and cyclic performance of the connection and can increase ductility and energy dissipation and increase the bending stiffness at the connection. The thickness of the end plate calculated on the basis of the rupture relations has a suitable value. The use of lower thickness causes the local buckling of end plate and the use of a higher thickness does not have much impact on bending capacity.
- The use of high strength bolts is essential in connection with the end plate. Otherwise, the bolts will yield, which is by no means desirable.
- The use of a double plate in cases where the column web is thin is necessary to prevent yielding in the panel zone.
- The use of a gusset plate leads to stress distribution in the end plate and column flange and improves the flexural capacity.
- The use of ST-52 steel for the end plate improves the flexural capacity.
- If the column flange is thin, the flexural connection cannot reach its maximum capacity, and minimum thickness observation for the column flange is mandatory.

- The degree of flexural and rotational stiffness of the connections, as well as the amount of absorbed energy increase in case of using continuity plate, double plate and gusset plate.

## REFERENCES

- [1] Grundy, P. and Bennetts, D. and Thomas, R., "Beam-to-Column Moment Connections", *Journal of the Structural Division, ASCE*, 1980, Vol. 106, pp.313-330.
- [2] Tsai, K.C. and Popov, E. P., "Cyclic Behavior Of End-Plate Moment Connections", *Journal of Structural Engineering, ASCE*, 1990, Vol. 116, pp.2917 – 2930.
- [3] Hejazi, M. and Mehdad, H., "Finite Element Analysis and the Effects of Strengthening end plate in beam - column Flanged connections", *Eighth International Civil Engineering Congress*, 2009, pp.2-7.
- [4] Joshi, p. and Solanki, J G., "Computational Modelling of Indian Standard Extended Endplate Moment Connection", *International Journal of Advanced Technology in Engineering and Science*, 2014, Vol.02, pp.417-424.
- [5] Rajeshkumar, B. and Dr. Yamini Sreevalli, I., "Behaviour of Bolted Endplate Connection under Elevated Temperature", *International Journal of Research in Civil Engineering, Architecture & Design*, 2013, vol.1, pp. 51-55.
- [6] Balci, R., "Numerical models of welded and bolted beam to column connections", *Acta Technica Napocensis: Civil Engineering & Architecture*, 2012, Vol. 55, pp.30-36.
- [7] Baei, M. and Ghassemieh, M. and Goudarzi, A., "Numerical Modelling of End-Plate Moment Connection Subjected to Bending and Axial Forces", *The Journal of Mathematics and Computer Science*, 2012, Vol. 4, pp.463 – 472.
- [8] Ismail, R. E. S. and Fahmy, A.S. and Khalifa, A. M. and Mohamed, Y. M., "Numerical Study on Ultimate Behaviour of Bolted End-Plate Steel Connections", *Latin American Journal of Solids and Structures*, 2016, Vol.13, pp.1-22.
- [9] Saberi, V. and Gerami, M. and Kheyroddin, A., "Comparison of bolted end plate and T-stub connection sensitivity to component thickness", *Journal of Constructional Steel Research*, 2014, vol. 98, pp.134–145.

- [9] Saberi, H. and Kheyroddin, A. and Gerami, M., "Comparison of bolted end plate and T-stub connections sensitivity to bolt diameter on cyclic behavior", *International journal of steel structures*, 2014, Vol.14, pp.633-647.
- [9] Saberi, H. and Kheyroddin, A. and Gerami, M., "Welded haunches for seismic retrofitting of bolted T-stub connections and flexural strengthening of simple connections", *Journal of Engineering structures*, 2016, Vol.129, pp.31-43.
- [9] Saberi, V. and Gerami, M. and Kheyroddin, A., "Seismic rehabilitation of bolted end plate connections using post-tensioned tendons", *Journal of Engineering structures*, 2016, Vol.129, pp.18-30.
- [10] Dessouki, A.K. and Youssef, A.H. and Ibrahim, M.M., "Behavior of I-beam bolted extended end-plate moment connections", *Ain Shams Engineering Journal*, 2013, Vol.4, pp.685-699.
- [11] Ghassemieh, M. and Nasseri, M., "Evaluation of Stiffened End-Plate Moment Connection through Optimized Artificial Neural Network", *Journal of Software Engineering and Applications*, 2012, vol.5, pp.156-167.
- [12] Chen, X. and Shi, G., "Finite element analysis and moment resistance of ultra-large capacity end-plate joints", *Journal of Constructional Steel Research*, 2016, Vol.126, pp.153-162.
- [13] Wang, M. and Shi, Y. and Wang, Y. and Shi, G., "Numerical study on seismic behaviors of steel frame end-plate connections", *Journal of Constructional Steel Research*, 2013, Vol.90, pp. 140-152.
- [14] Saberi, H. and Kheyroddin, A. and Gerami, M., "Seismic Strengthening of Weak Bolted End Plate connections Using Welded Haunches", *International Journal of Steel Structures*, 2017, Vol.17, pp.1-13.
- [15] Gerami, M. and Saberi, H. and Saberi, V. and Saedi Daryan, A., "Cyclic behavior of bolted connections with different arrangement of bolts", *Journal of Constructional Steel Research*, 2011, Vol.67, pp.690-705.
- [16] Saedi Daryan, A. and Sadri, M. and Saberi, H. and Saberi, V. and Baleh Moghadas, A., "Behavior of semi-rigid connections and semi-rigid frames", *Journal of the structural Design of tall and special Buildings*, 2012, Vol.23, pp.210-238.
- [16] Saberi, H. and Kheyroddin, A. and Gerami, M. and Karimlu, M., "Rotational capacity of castellated steel beams", *Journal of The Structural Design of Tall and Special Buildings*, 2013, Vol.22, pp.941-953.
- [17] Guo, B. and Gu, Q. and Liu, F., "Experimental Behavior of Stiffened and Unstiffened End-Plate Connections under Cyclic Loading", *Journal of Structural Engineering* © ASCE, 2006, Vol.132, pp.1352-1357.